ARL-TR-9451 ● APR 2022

DEVCOM ARMY RESEARCH LABORATORY

# X-Ray Computed Tomography Evaluation of Electron Beam Additively Manufactured Titanium Components

by William Green

## NOTICES

### Disclaimers

The findings in this report are not to be construed as an official Department of the Army position unless so designated by other authorized documents.

Citation of manufacturer's or trade names does not constitute an official endorsement or approval of the use thereof.

Destroy this report when it is no longer needed. Do not return it to the originator.

ARL-TR-9451 ● APR 2022


# X-Ray Computed Tomography Evaluation of Electron Beam Additively Manufactured Titanium Components

**William Green**
*DEVCOM Army Research Laboratory*

# REPORT DOCUMENTATION PAGE

*Form Approved*
*OMB No. 0704-0188*



| 1. REPORT DATE *(DD-MM-YYYY)* | 2. REPORT TYPE | 3. DATES COVERED (From - To) |
|---|---|---|
| April 2022 | Technical Report | 1 June–17 September 2021 |

**4. TITLE AND SUBTITLE**
X-Ray Computed Tomography Evaluation of Electron Beam Additively Manufactured Titanium Components

**5a. CONTRACT NUMBER**

**5b. GRANT NUMBER**

**5c. PROGRAM ELEMENT NUMBER**

**6. AUTHOR(S)**
William Green

**5d. PROJECT NUMBER**

**5e. TASK NUMBER**

**5f. WORK UNIT NUMBER**

**7. PERFORMING ORGANIZATION NAME(S) AND ADDRESS(ES)**
DEVCOM Army Research Laboratory
ATTN: FCDD-RLW-MB
Aberdeen Proving Ground, MD 21005

**8. PERFORMING ORGANIZATION REPORT NUMBER**
ARL-TR-9451

**9. SPONSORING/MONITORING AGENCY NAME(S) AND ADDRESS(ES)**
DEVCOM GVSC - Detroit Arsenal
6501 E Eleven Mile Rd
Warren, MI 48397-0001

**10. SPONSOR/MONITOR'S ACRONYM(S)**
DEVCOM GVSC

**11. SPONSOR/MONITOR'S REPORT NUMBER(S)**

**12. DISTRIBUTION/AVAILABILITY STATEMENT**
Approved for public release: distribution unlimited.

**13. SUPPLEMENTARY NOTES**
ORCID ID: William Green, 0000-0001-8772-3946

**14. ABSTRACT**
Two electron beam additively manufactured (EBAM) titanium specimens provided by the US Army Combat Capabilities Development Command Ground Vehicle Systems Center at the Tank-Automotive and Armaments Command, Detroit Arsenal, were inspected and evaluated using X-ray computed tomography (XCT). XCT scanning parameters and overall protocols used to achieve acceptable scan image results are discussed. XCT image results, including 2-D internal slices at select locations and 3-D sectioned visualizations, are also shown and discussed. The physical nature of the types of features found in these specimens are also described and discussed.

**15. SUBJECT TERMS**
additive manufacturing, AM, electron beam AM, EBAM, X-ray computed tomography, XCT, discontinuity, lap, separation, Sciences of Extreme Materials

| 16. SECURITY CLASSIFICATION OF: | | | 17. LIMITATION OF ABSTRACT | 18. NUMBER OF PAGES | 19a. NAME OF RESPONSIBLE PERSON |
|---|---|---|---|---|---|
| a. REPORT | b. ABSTRACT | c. THIS PAGE | | | William Green |
| Unclassified | Unclassified | Unclassified | UU | 30 | 19b. TELEPHONE NUMBER (Include area code) (410) 306-0817 |

Standard Form 298 (Rev. 8/98)
Prescribed by ANSI Std. Z39.18

## Contents

## List of Figures



## List of Tables

## 1. Introduction

The X-ray computed tomography (XCT) technique is a widely applicable and powerful nondestructive inspection modality for evaluation and analysis of geometrical and physical characteristics of materials, especially internal structures and features. XCT is applicable to metals, ceramics, plastics, and polymer and mixed composites, as well as components, assemblies, and materiel. The principal advantage of XCT is that it provides densitometric (that is, radiological density and geometry) images of thin cross sections through an object in a noninvasive manner. Because of the absence of structural superimposition, images are much easier to interpret than conventional radiological images. The user can quickly learn to read XCT data because images more closely correspond to the way the human mind visualizes 3-D structures than 2-D projection radiology (that is, film radiography, real-time radiography, and digital radiography).[1–4] The Weapons and Materials Research Directorate (WMRD) of the US Army Combat Capabilities Development Command Army Research Laboratory has identified additive manufacturing (AM) of certain materials and components as an essential research area. Metals AM with an emphasis on high-strength steel alloys, among other areas like titanium alloys, is an applied research and development (R&D) area of the Sciences of Extreme Materials Division (SEMD) in WMRD.

XCT is an excellent nondestructive evaluation (NDE) method for inspecting these relatively dense and oftentimes geometrically complex materials. Two electron beam AM (EBAM) titanium specimens provided by the US Army Combat Capabilities Development Command Ground Vehicle Systems Center (GVSC) at Tank-automotive and Armaments Command, Detroit Arsenal, were inspected and evaluated by XCT. XCT scanning parameters and overall protocols used to achieve acceptable scan image results are described in Section 3. Section 4 shows and discusses the XCT image results, including 2-D internal slices at select locations and 3-D sectioned visualizations exposing internal surfaces. The physical nature of the types of features found in these specimens are also discussed.

## 2. Specimen Description

The EBAM titanium specimens included a smaller rectangular piece sectioned from a larger block and a much larger sectioned half ring. The overall dimensions of the rectangular specimen were approximately 3 × 1.19 × 0.88 inches (76.2 × 30.2 × 22.4 mm). The uncut face of the specimen was part of the outside surface of the larger block and was very uneven. It was known that the specimen had a feature of interest in its uncut face before XCT scanning took place. The sectioned half ring

had a diameter of about 17 inches with a wall height of about 5 inches and varying thickness from about 0.5 to 1 inches. The half-ring specimen was significantly more difficult to scan and produce fair XCT results due to its very large diameter and 5-inch wall height, as well as its arcing shape.

# 3. XCT Scan Methods

## 3.1 Sectioned Rectangular Specimen

The specimen was secured within a free-standing foam base to stabilize it on the scanning turntable such that its areal faces were approximately vertical. Its top and bottom end surfaces were approximately horizontal. The parameters of the XCT technique used to scan the specimen are given in Table 1. Parameters in the table exhibit scanning process steps taken to maximize signal-to-noise ratio (SNR) and image quality while minimizing noise and high X-ray attenuation artifacts, including X-ray beam hardening (source filter), frame averaging, and view (i.e., projection) oversampling.

**Table 1 XCT scanning parameters for rectangular specimen**

| Parameter | Value |
|---|---|
| X-ray voltage (peak) | 450 kV |
| X-ray energy (peak) | 450 keV |
| X-ray current | 1410 µA |
| Detector sample rate | 4 frame/s (fps) |
| X-ray focal spot size | 400 µm |
| Source-to-image distance | 890 mm |
| Source-to-object distance | 593 mm |
| Magnification | 1.5 |
| Detector element pitch | 200 µm |
| Effective pixel pitch | 133 µm |
| Unsharpness | 1.0 pixels |
| Frame average | 4 |
| No. projections (views) | 475 |
| Source filter (copper) | ≈1.59 mm (0.063 inch) |
| Detector filter (lead) | ≈.127 mm (0.005 inch) |

## 3.2 Sectioned Half-Ring Specimen

The half-ring specimen was XCT scanned two times because the first scan was of relatively low quality. In the first scan the half ring was oriented with its axial direction tilted from vertical a relatively small number of degrees. Thus, the radial direction was tilted the same amount from horizontal. It is likely that relatively long X-ray paths through arc sections of the half ring in this orientation resulted in very

high attenuation and significant lack of X-ray intensity at the detector, resulting in very compromising "black air" artifacts in the reconstructed image data. For this reason, the half ring was rescanned with its axial and radial directions approximately horizontal and vertical, respectively. The half ring was stably secured in a bucket in this orientation using foam. X-rays were still highly attenuated by about 5 inches of titanium in certain ranges of turntable rotation positions, but the specimen orientation in the second scan resulted in higher quality reconstructed image data with less black air artifacts. The parameters of the XCT technique used to scan the specimen are given in Table 2. Parameters in the table exhibit scanning process steps taken to maximize SNR and image quality while minimizing noise and high X-ray attenuation artifacts, including X-ray beam hardening (source filter), frame averaging, and view (i.e., projection) oversampling.

**Table 2 XCT scanning parameters for half-ring specimen**

| Parameter | Value |
|---|---|
| X-ray voltage (peak) | 450 kV |
| X-ray energy (peak) | 450 keV |
| X-ray current | 1380 μA |
| Detector sample rate | 2 frame/s (fps) |
| X-ray focal spot size | 400 μm |
| Source-to-image distance | 1250 mm |
| Source-to-object distance | 875 mm |
| Magnification | 1.43 |
| Detector element pitch | 200 μm |
| Effective pixel pitch | 140 μm |
| Unsharpness | 0.86 pixels |
| Frame average | 4 |
| No. projections (views) | 2160 (helical) |
| Source filter (copper) | ≈1.59 mm (0.063 inch) |
| Detector filter (copper) | ≈1.59 mm (0.063 inch) |

# 4. XCT Scan Results and Discussion

## 4.1 Sectioned Rectangular Specimen

3-D densitometric XCT image data sets provide a very powerful and unique method to directly visualize, interpret, and evaluate internal structure and features in materials. Figure 1 shows outside surface views of the uncut face of the specimen with the slanted right-hand image showing the thickness of it. Figure 2 shows the same views as in Fig. 1 with the feature of interest identified in both images. Figures 3a–c show a set of 2-D planar views located through the specimen in the thickness direction. Figure 3a is very close to the uncut and overall uneven surface

of the specimen and the images of Figs. 3b and c are deeper into it. Figures 4a–h show a series of 3-D sectioned images and 2-D planar views located through the specimen in the width direction (side-to-side) beginning closest to the left side, which is the side the lap or flap feature is on. Figures 4a and b are a matched 3-D sectioned and 2-D planar image pair, as are Figures 4c and d, in which the 3-D sectioned image and 2-D planar view are on the left-hand (4a and c) and right-hand (4b and d) sides of the pair, respectively. The 3-D sectioned views, which display unremoved, visible surface area, are shown for comparison to their corresponding 2-D planar views on the right in Figs. 4b and d. Figures 4e–h are all 2-D planar views moving farther and farther in the width direction. The images show how the lap, which is characterized by the arc shaped crack or missing material underneath it, changes as the images move across it from one side to the other. Figure 5 shows a 3-D sectioned view and its corresponding 2-D planar view of a separate small crack-like feature in the surface of the specimen. Figures 6a–k show a series of 3-D sectioned images and 2-D planar views located through the specimen in the height direction (top to bottom) beginning near the top of the lap. Figures 6a and b are a matched 3-D sectioned and 2-D planar image pair, as are Figs. 6c and d, in which the 3-D sectioned image and 2-D planar view are on the left-hand (6a and c) and right-hand (6b and d) sides of the pair, respectively. The 3-D views are again shown for comparison to their corresponding 2-D views on the right in Figs. 6b and d. Images in Figs. 6e–k are all 2-D planar views moving through the lap from top to bottom in the height direction. The images show how the lap, which is again characterized by the arc-shaped crack or missing material underneath it, changes as the images move across it from the top to the bottom. This series of images also clearly shows that the lap has more than one “petal” with multiple cracks underneath it. Figure 7 shows sections of five different 2-D planar images giving the approximate overall depth and width dimensions of different areas of the lap. From these images the maximum dimensions of the lap are approximately 0.17 (wide) × 0.33 (long) × 0.091 (deep) inches (4.4 × 8.3 × 2.3 mm).

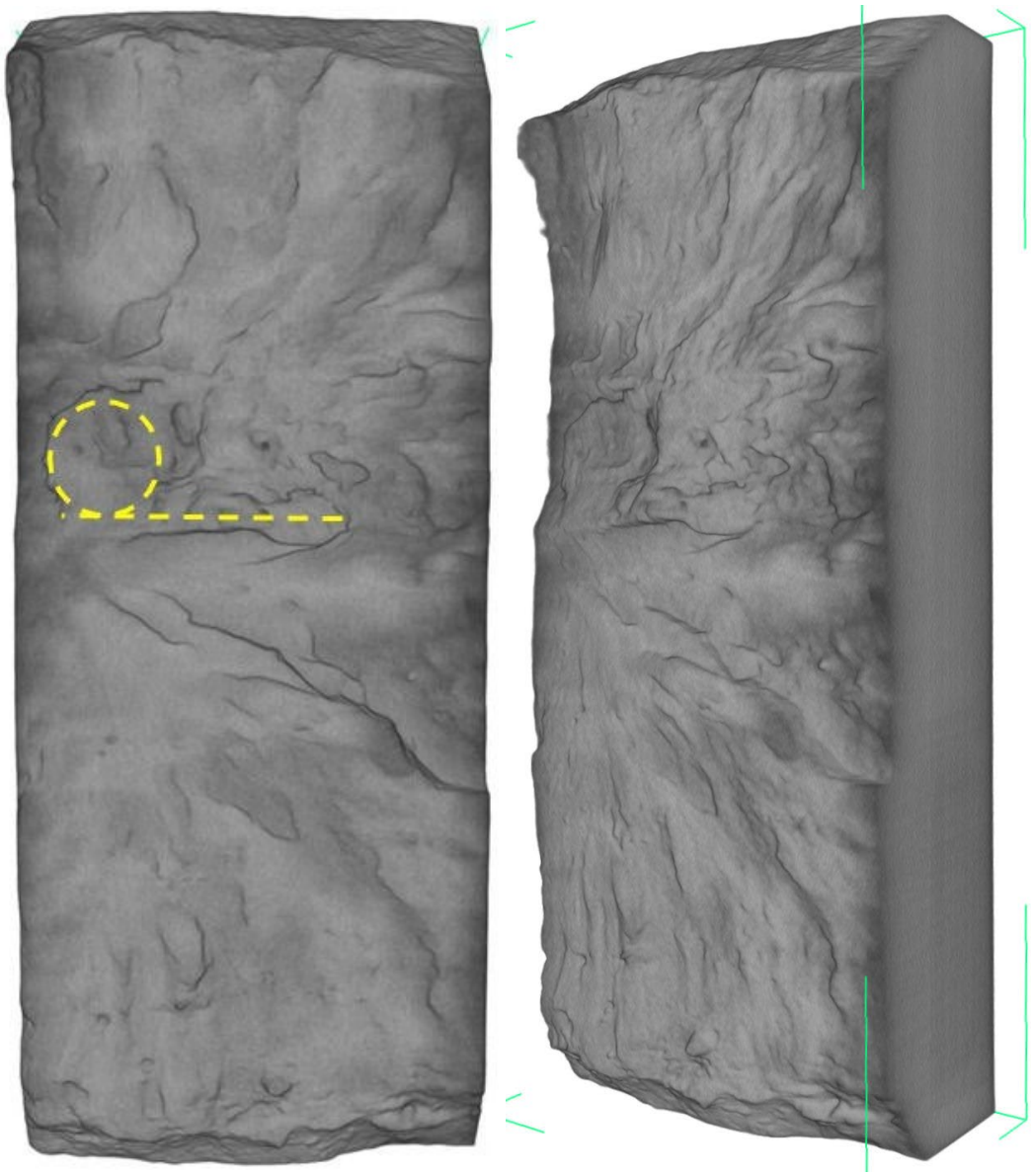

**Fig. 1 Views of outside uncut surface of sectioned rectangular specimen. Location and orientation of general "P" shape in surface of specimen is shown by dashed yellow lines in image on the left.**

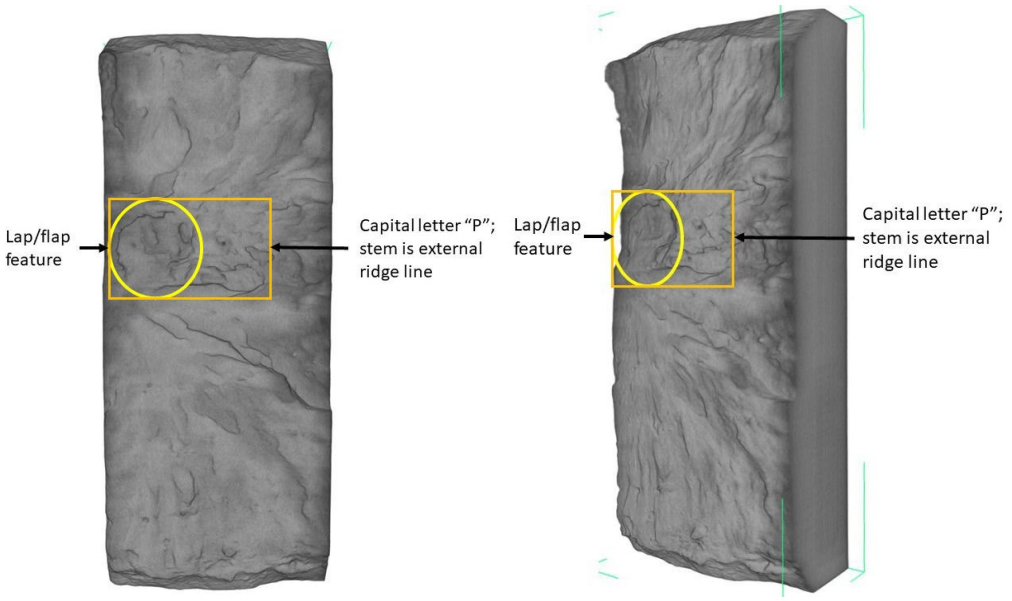


**Fig. 2 Views of outside surface of specimen with feature of interest identified**

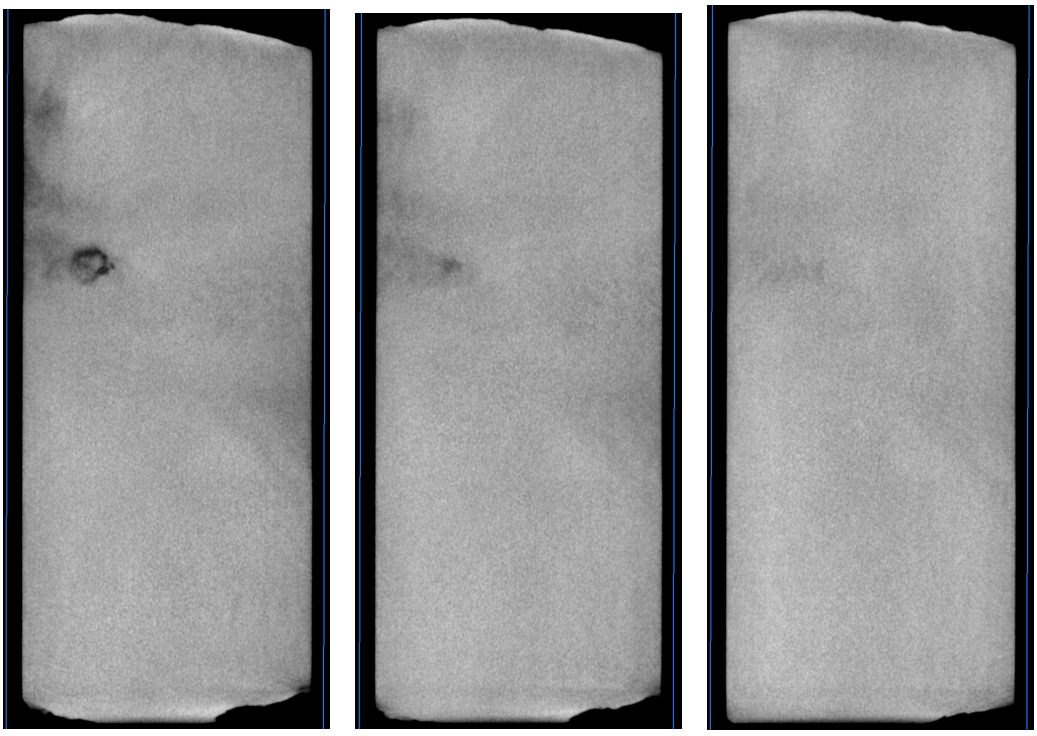


**Fig. 3 A set of 2-D planar images located through the specimen in the thickness direction**

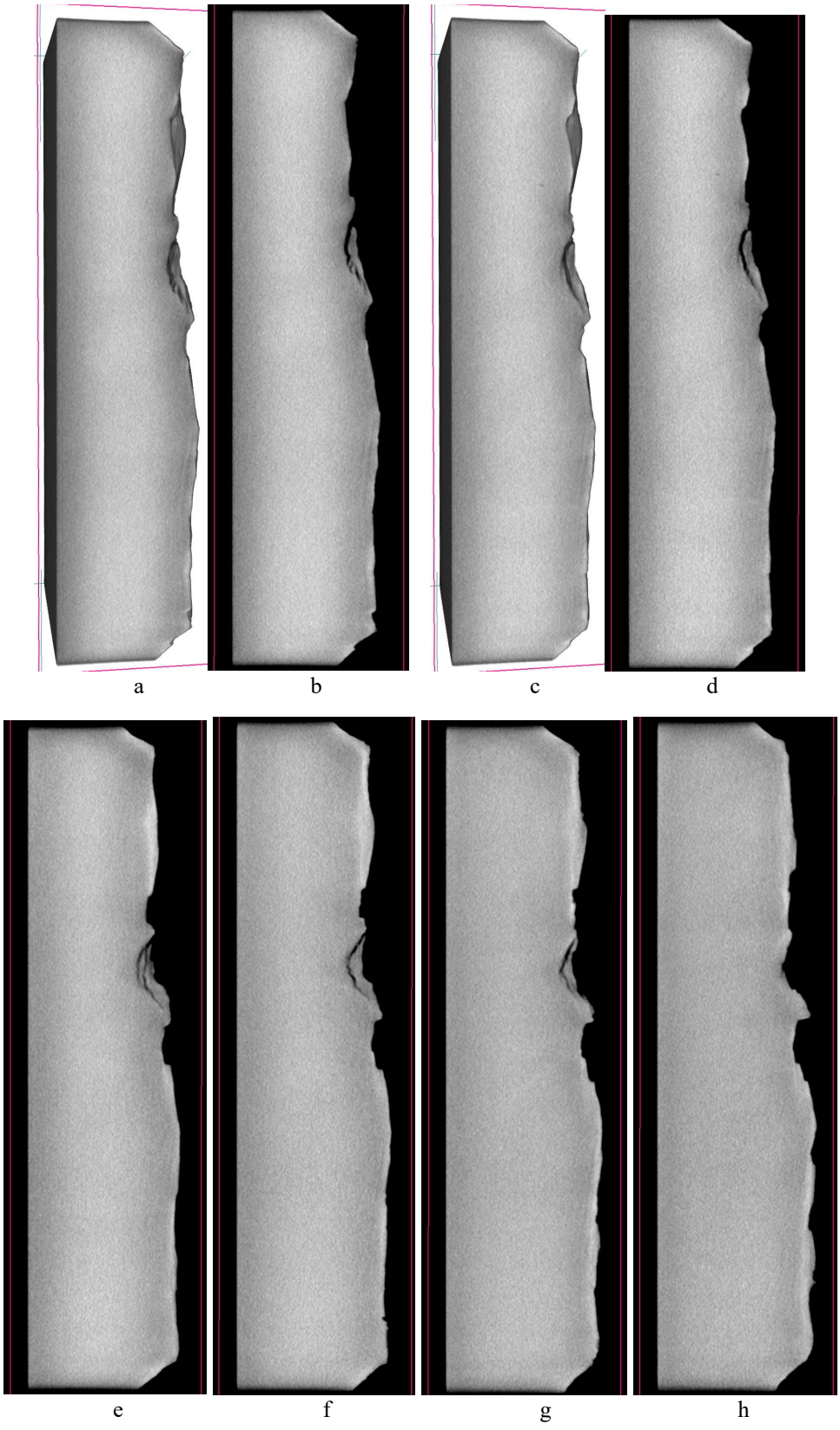


**Fig. 4 (a and c) 3-D sectioned and (b, d, and e–h) 2-D planar images located through the specimen in the width direction (side-to-side)**

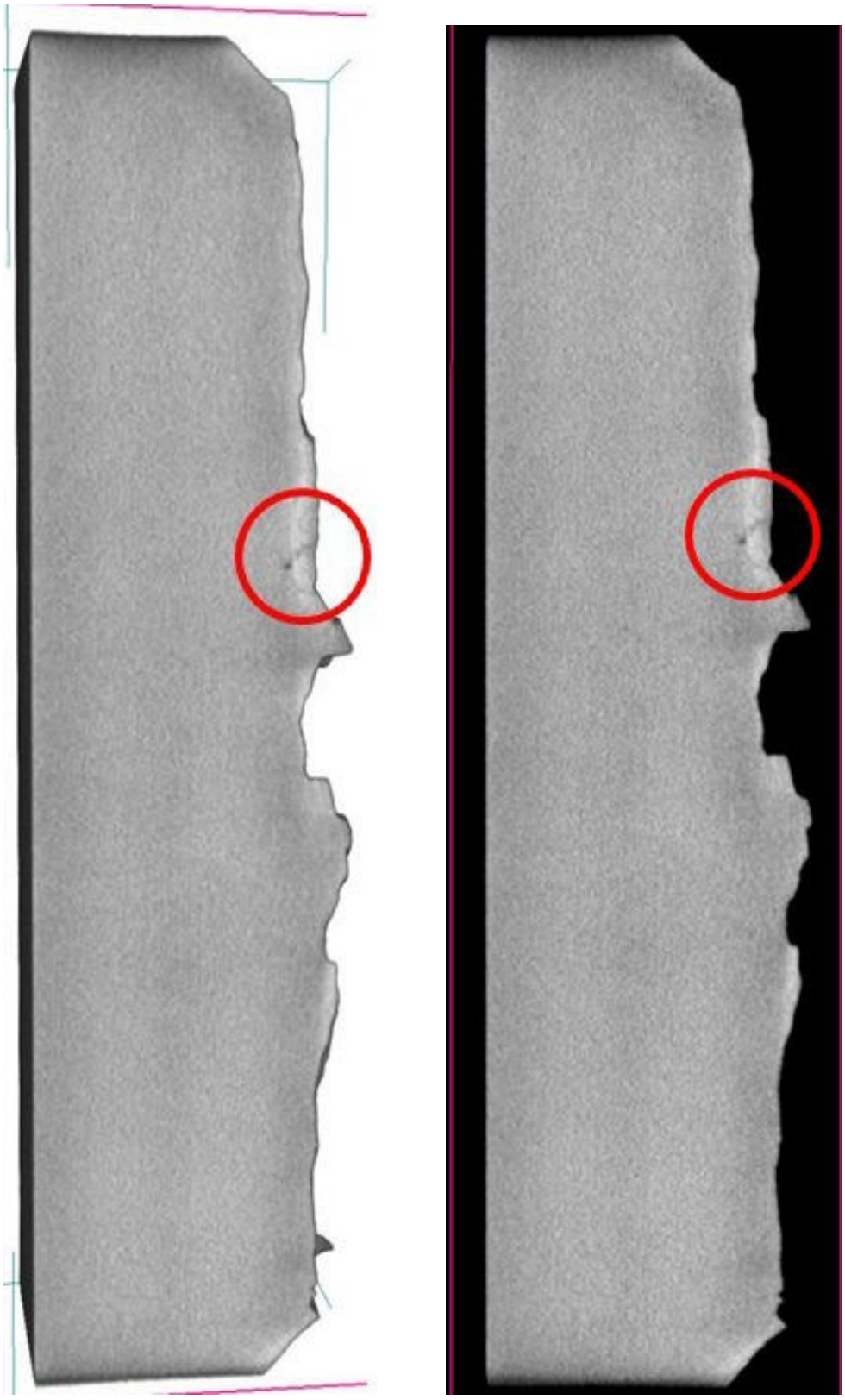

**Fig. 5 3-D sectioned (left) and 2-D planar (right) images of a separate small crack like discontinuity circled in red**

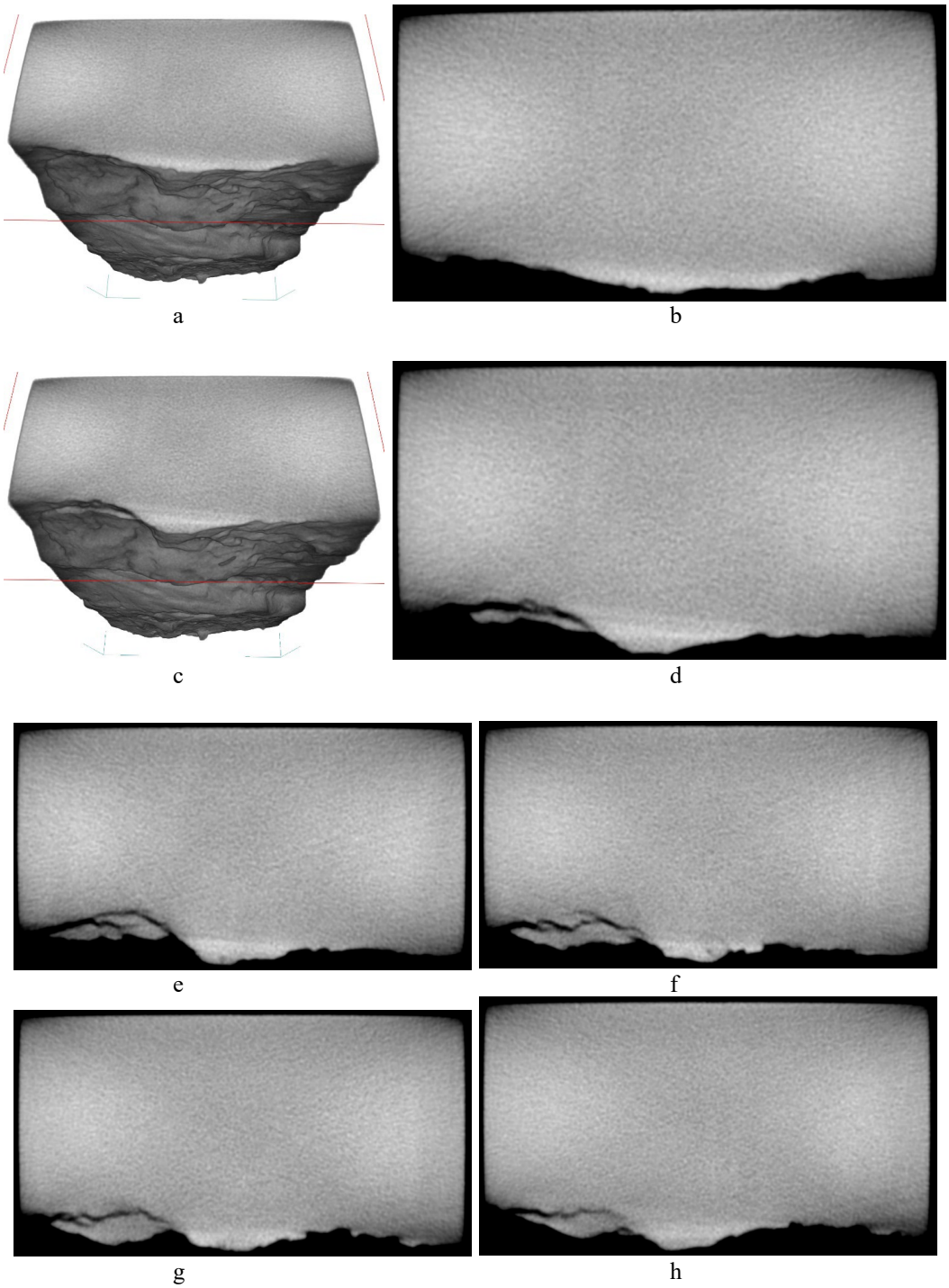


**Fig. 6 (a and c) 3-D sectioned and (b, d, and e–k) 2-D planar images located through the specimen in the height direction (top to bottom)**

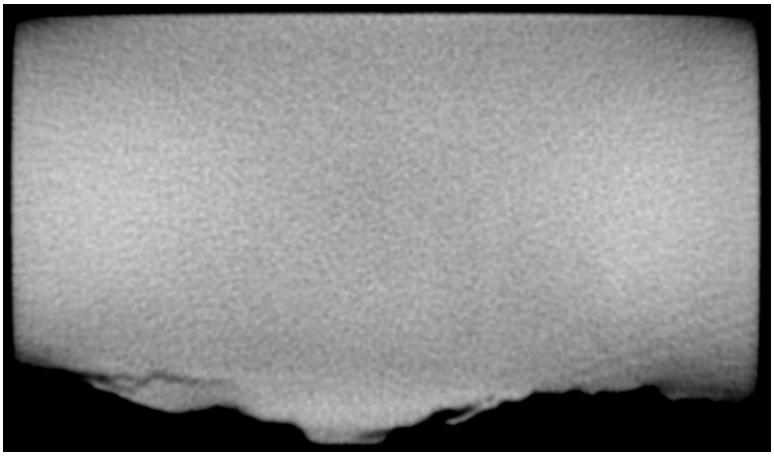

j

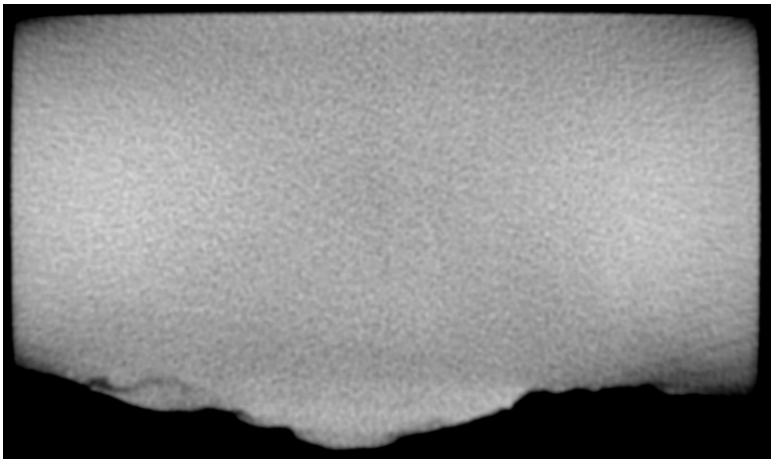

j

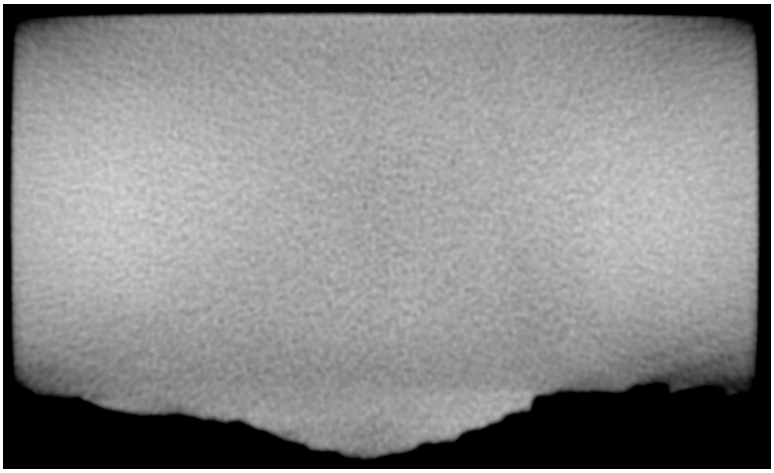

k

**Fig. 6 (a and c) 3-D sectioned and (b, d and e–k) 2-D planar images located through the specimen in the height direction (top to bottom) (continued)**

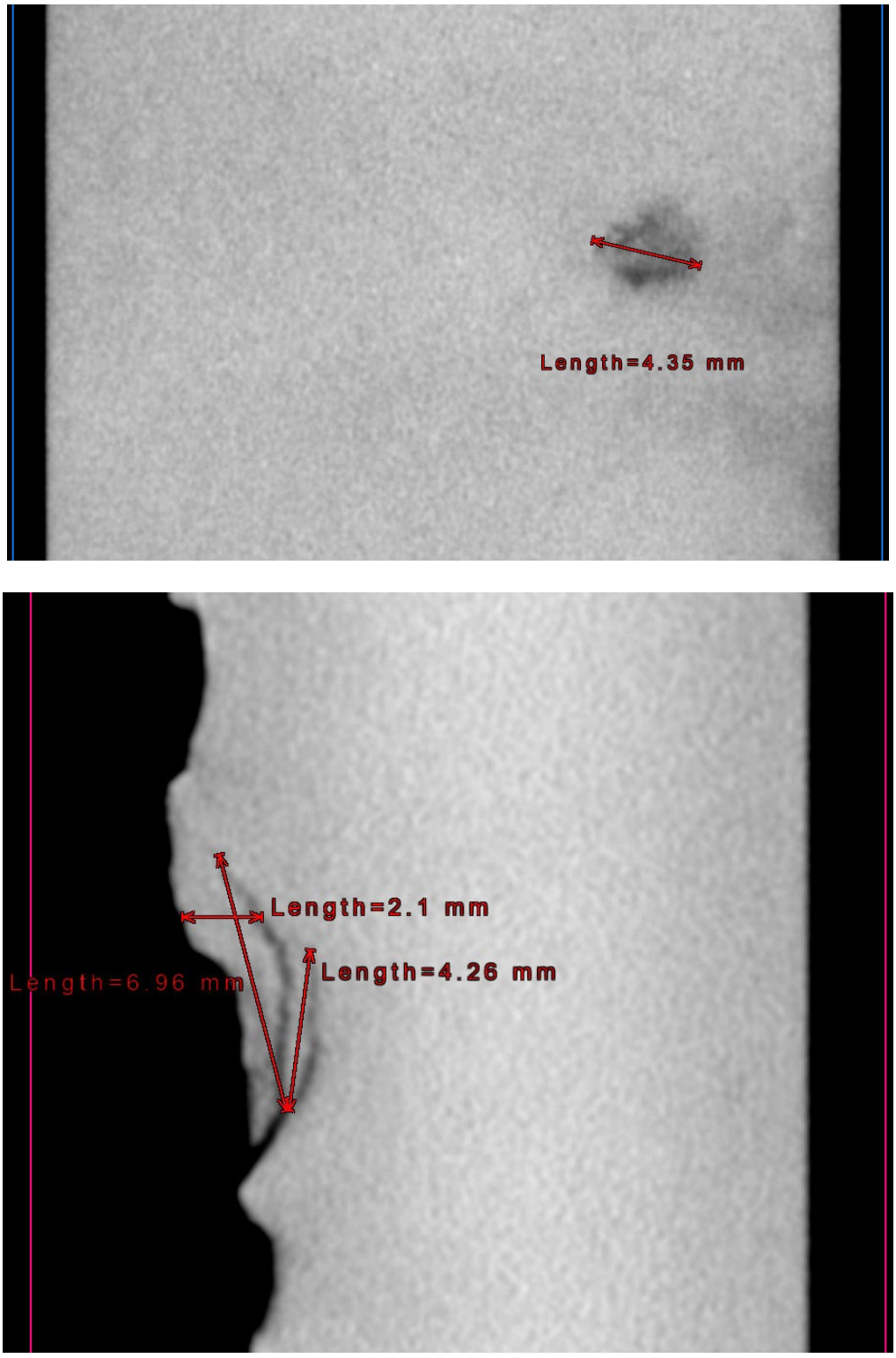


**Fig. 7 A series of close-ups of 2-D planar images giving approximate overall dimensions (e.g., areal length = 4.35 mm, distances from the surface, and crack origin to end tip lengths) of different areas of the lap**

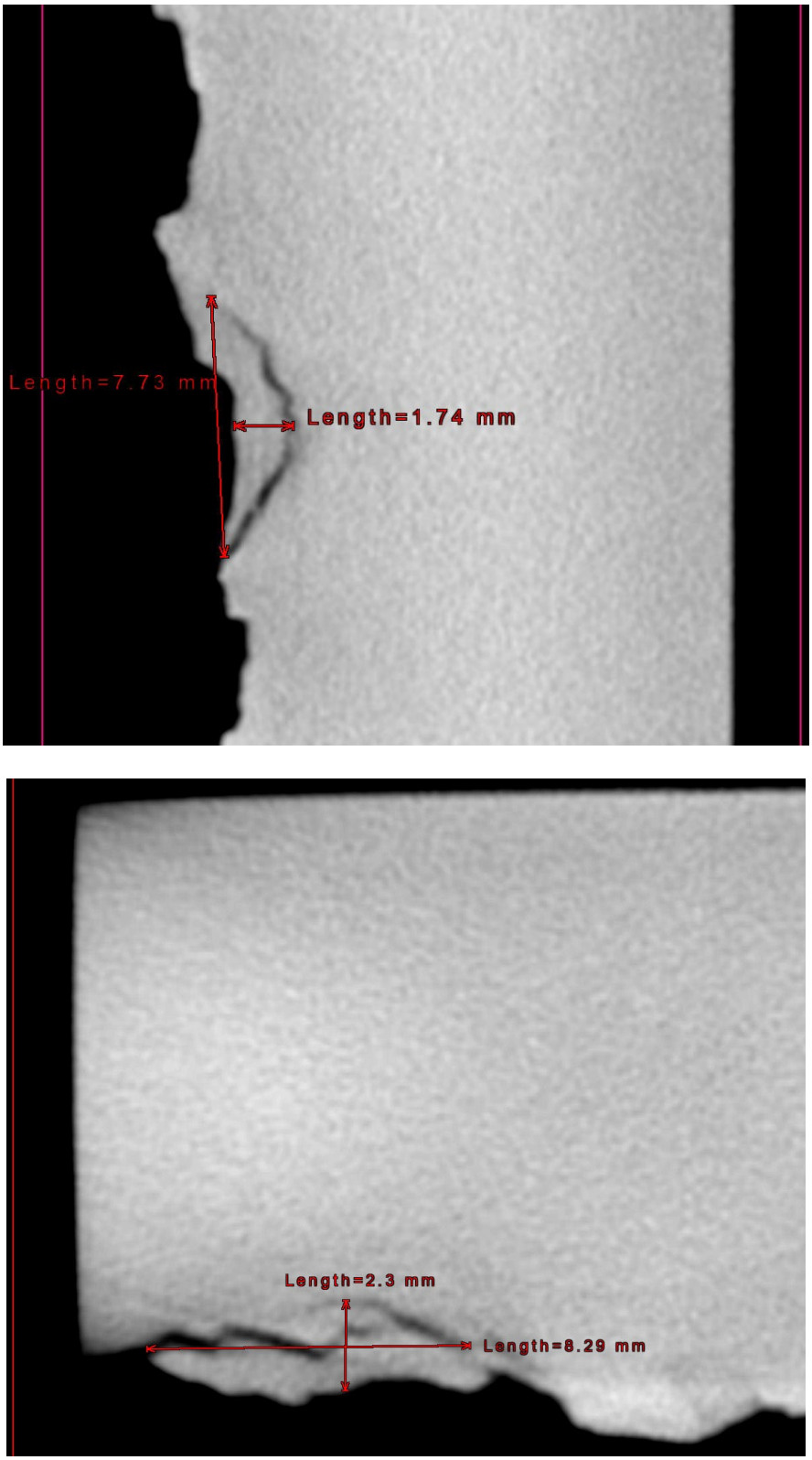


**Fig. 7 A series of close-ups of 2-D planar images giving approximate overall dimensions (e.g., areal length = 4.35 mm, distances from the surface, and crack origin to end tip lengths) of different areas of the lap (continued)**

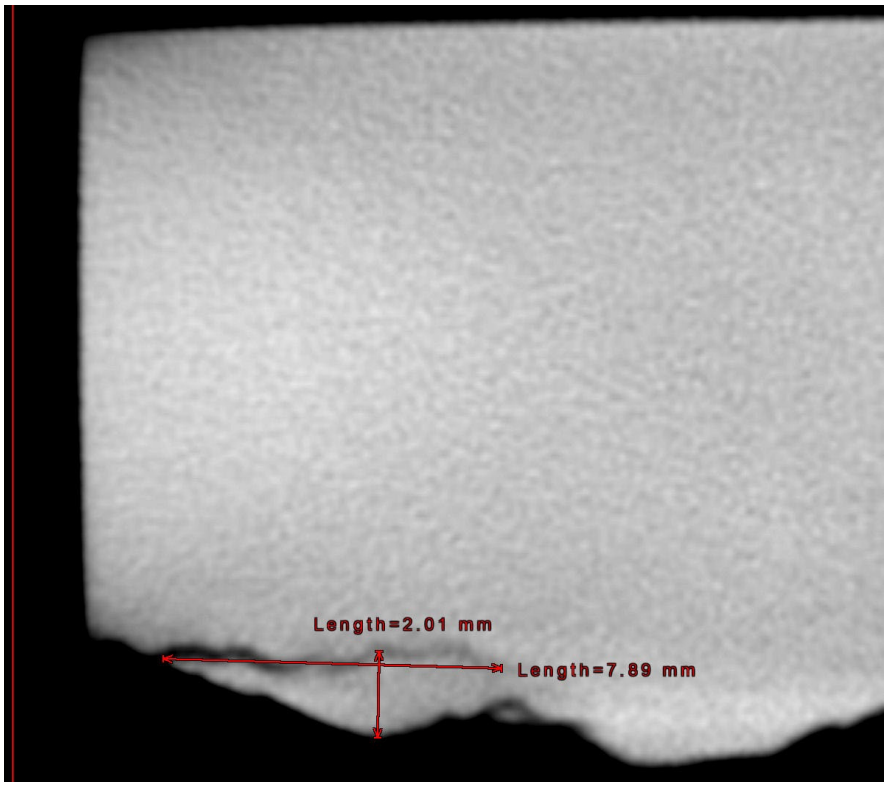


**Fig. 7 A series of close-ups of 2-D planar images giving approximate overall dimensions (e.g., areal length = 4.35 mm, distances from the surface, and crack origin to end tip lengths) of different areas of the lap (continued)**

## 4.2 Sectioned Half-Ring Specimen

Results from the first scan of the specimen are not discussed due to their relative lack of quality, except to say that highly attenuating path lengths through arc sections of the specimen produced very compromising air artifacts in the reconstructed image data that made it difficult, if not impossible, to interpret both interior and exterior features of the specimen. The second scan of the specimen did produce better image results, although there was still some level of the black air artifact in the images. Figure 8 shows an outside view of the half ring, in which some of the dark air artifact is apparent in the middle area of the half ring from one end to the other, along with a little more at the bottoms of the ends. Figures 9–11 show three sets of 3-D solid sectioned visualizations and their corresponding 2-D planar views. The 2-D view of Fig. 9 (middle image) appears to show a few relatively short gap-like features along the lower curved edge of the specimen. The bottom image of Fig. 9 is a close-up view of the middle image showing a smaller section in the middle and to the left. The relatively thin gaps in the lower side of the half ring, which are about 2–3 mm wide, are evident and highlighted by the

surrounding boxes and arrows. The 2-D view or slice of Fig. 9 is about 16 mm from the top of the thinner wall section of the half ring, which is facing up toward the viewer in the perspective of the images. Physical sectioning of the half ring was only done parallel to the height direction and essentially along radial lines and not in any planes parallel to the 2-D slices in Fig. 9. Sectioning did not reveal any gap features similar to those in Fig. 9. The presence of these short gaps may be due to an undulating vertical surface (height direction) with thin overlaps or overhangs that have air between them and the main body of the half ring. This could explain the gap-like appearance of these features. However, given the single titanium material pass procedure of the AM build process throughout the height of the half ring, except in the flange section, it is unclear how these gaps could have formed as they are not in the flange section. The darker vertical banding at the ends of the half ring in Fig. 10 is an image artifact. However, the material along the upper curved area appears to have striations in it. Figure 12 shows a set of 3-D solid and 2-D planar front views. Figures 13a–d show a series of 2-D planar views that section the half ring at various locations. Unfortunately, the overall size, shape, and dimensions of the half ring resulted in uneven gray level variation over relatively large areas in these images. These effects, as well as the darker diagonal band from one side of the half ring to the other, are not due to physical differences in the specimen. In Figs. 13a–d the so-called striations in the horizontal part of the half ring appear to be due to streaking artifacts. However, the various images in all the figures do not show porosity, cavities, cracks, or inclusions in the titanium material, except for the few small gaps in Fig. 9.

**Fig. 8 Outside 3-D solid image of the half-ring specimen, in which some of the dark air artifact is apparent in the middle area of the half ring from one end to the other**

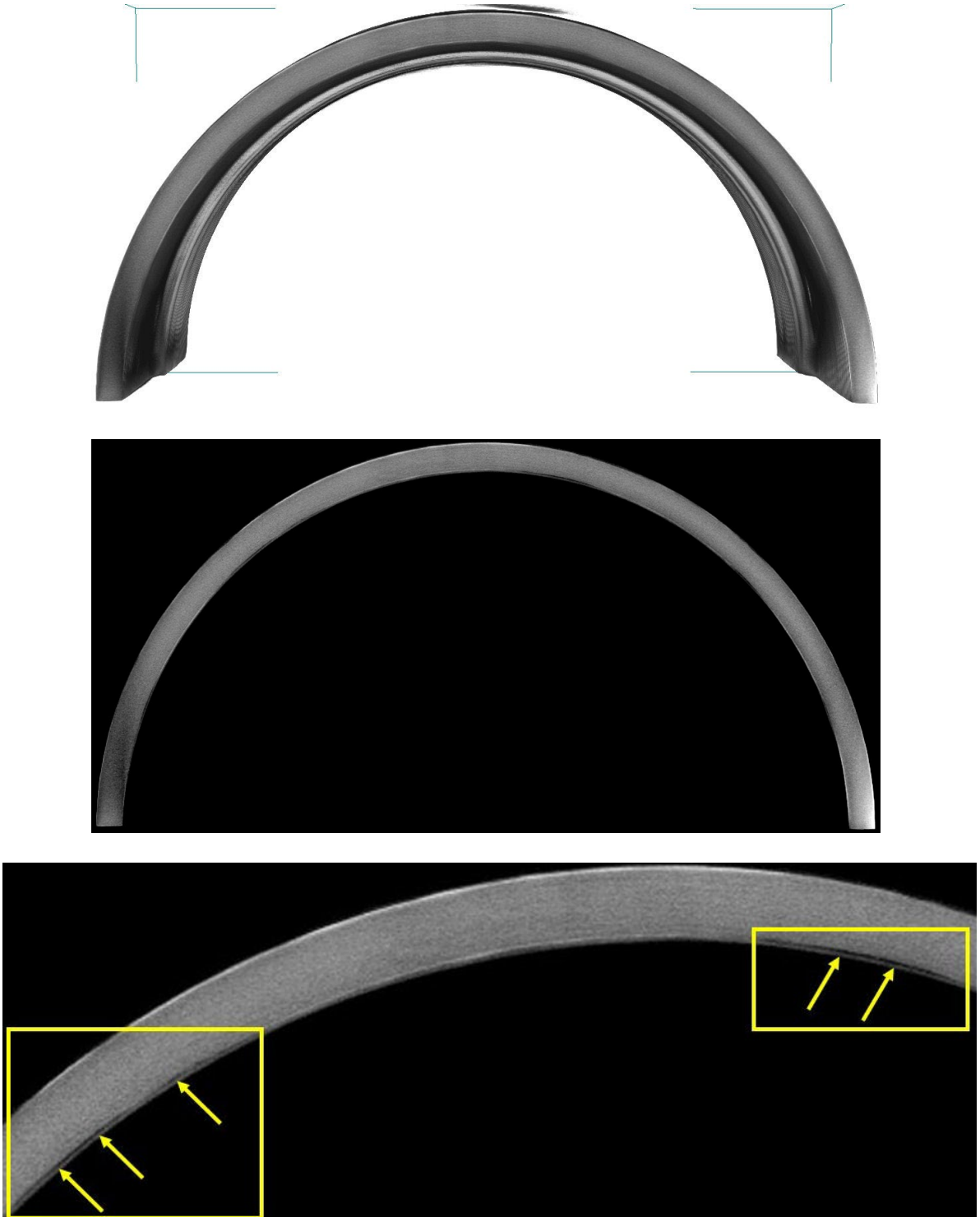

**Fig. 9 First set of 3-D solid sectioned visualizations (top image) and their corresponding 2-D planar images in the height (top to bottom) direction. 2-D planar image (middle) and a close-up view (bottom) of a smaller section of middle image.**

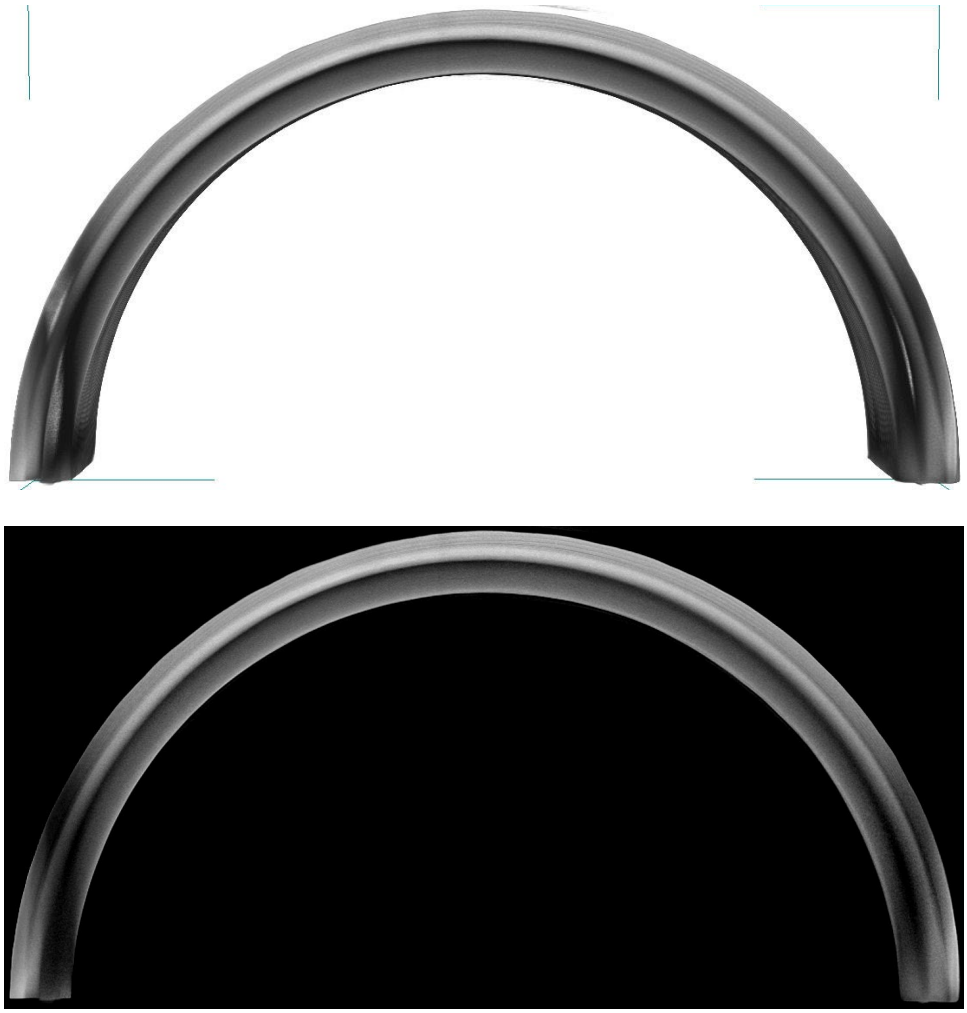

**Fig. 10 Second set of 3-D solid sectioned visualizations (top image) and their corresponding 2-D planar (bottom image) images in the height (top to bottom) direction**

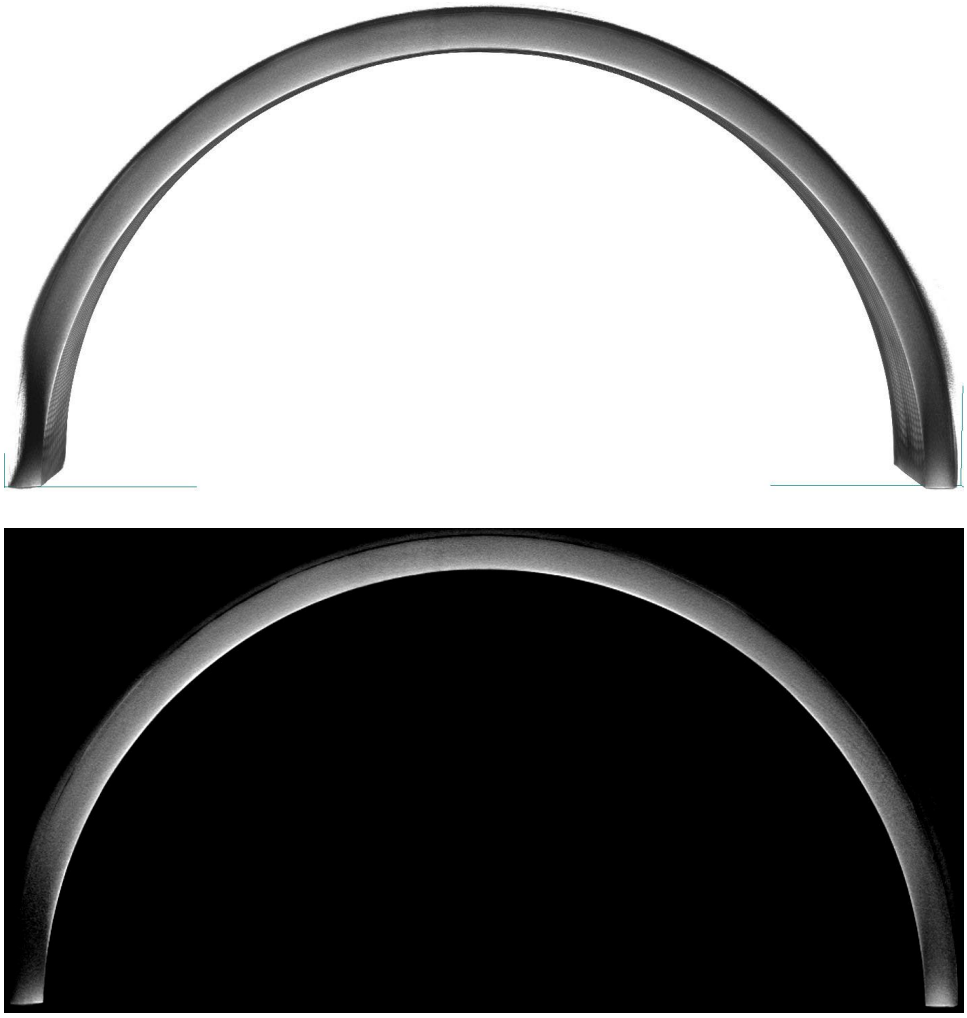

**Fig. 11 Third set of 3-D solid sectioned visualizations (top image) and their corresponding 2-D planar (bottom image) images in the height (top to bottom) direction**

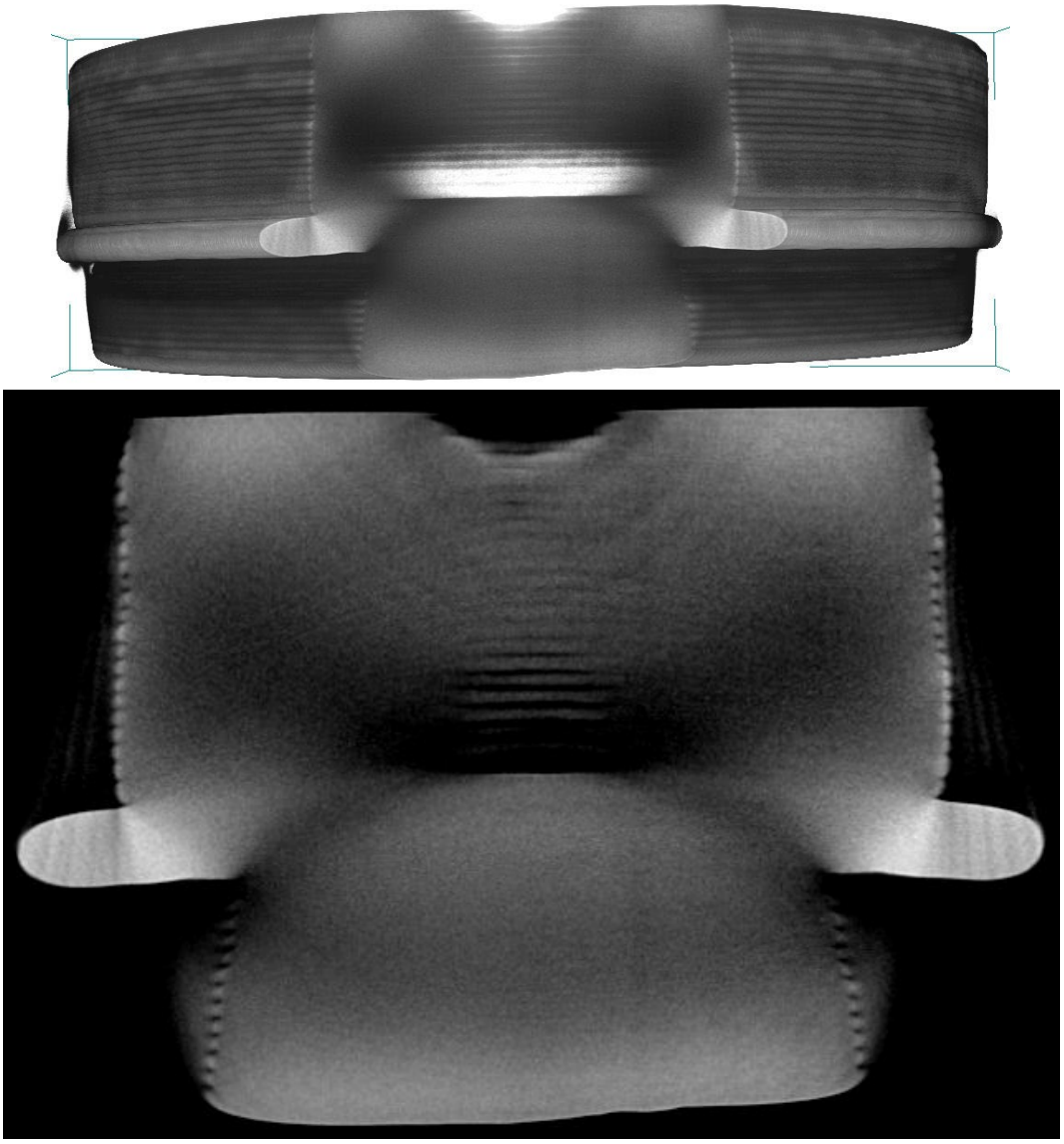

**Fig. 12 Set of 3-D solid section (top image) and corresponding 2-D planar front view (bottom image) images in the front to back direction**

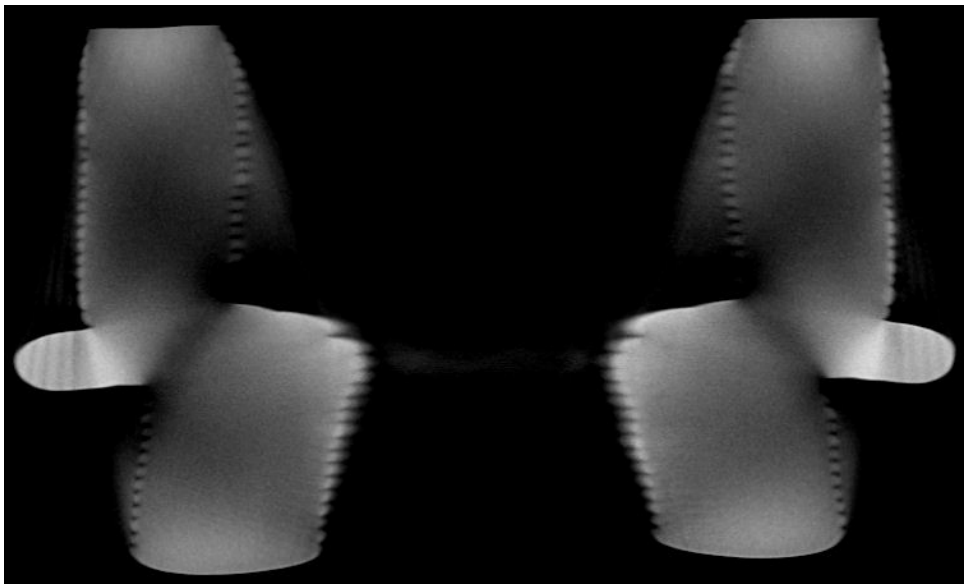

a

b

c

**Fig. 13 (a–d) A series of 2-D planar images that section the half ring at various locations in the radial or side-to-side direction**

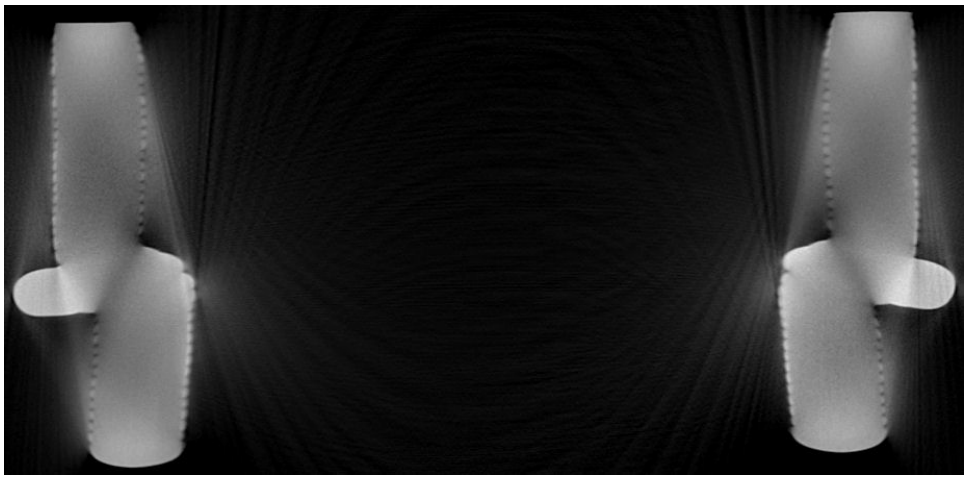

d

**Fig. 13 (a–d) A series of 2-D planar images that section the half ring at various locations in the radial or side-to-side direction (continued)**

## 5. Conclusion

Two different EBAM titanium specimens were received from DEVCOM GVSC and inspected using XCT. The smaller specimen was a rectangular piece sectioned from a larger block and had one major discontinuity, which was a lap in the outside uncut face of the specimen. The crack or air space underneath the lap that defined it had maximum dimensions of approximately 0.17 (wide) × 0.33 (long) × 0.091 (deep) inches (4.4 × 8.3 × 2.3 mm). The larger specimen was a half ring sectioned from a full ring with dimensions of approximately 17 inches in diameter with a wall height of about 5 inches and varying thickness from about 0.5 to 1 inches. The specimen had to be XCT scanned a second time in a different way in order to produce fair quality reconstructed image data. Even though the image data exhibited some artifacts because of X-ray attenuation effects due to the overall size, shape, and dimensions of the specimen, it did not appear to have any detectable porosity, cracks, cavities, or inclusions in the material. The exception is what appeared to be a few relatively short gaps about 2–3 mm wide along the inside circumference of the specimen. Given the single titanium material pass procedure of the AM build process throughout the height of the half ring, except in the flange section, it is unclear how these gaps could have formed as they are not in the flange section. Otherwise, the half ring appeared to be free of detectable discontinuities.

Given the effective pixel pitch of these scans (133 and 140 μm), discontinuities with overall dimensions less than about 0.25 mm were likely not detectable. However, XCT is a suitable NDE method for inspecting and characterizing EBAM materials of this size for mesoscale (i.e., sub-millimeter and usually well below 0.5 mm) flaws. Even better spatial resolution less than 0.25 mm can be achieved

with smaller specimens. The SEMD Materials Reliability and Design Branch will continue working with the GVSC to foster further XCT work supporting EBAM programs in the near future.

## 6. References


1. ASTM E 1570-95a. Standard practice for computed tomographic (CT) examination. ASTM International; 1995.
2. Dennis MJ. Industrial computed tomography: nondestructive evaluation and quality control. In: ASM handbook. Vol. 17. American Society for Metals (ASM) International; 1989.
3. Newton TH, Potts DG, editors. Technical aspects of computed tomography. In: Radiology of the skull and brain. Vol. 5. The CV Mosby Company; 1981.
4. Stanley JH. Physical and mathematical basis of CT imaging. American Society for Testing and Materials (ASTM), ASTM CT Standardization Committee (E7.01.07), ASTM Tutorial: Section 3; 1986.

## List of Symbols, Abbreviations, and Acronyms

| | |
|---|---|
| 2-D | two-dimensional |
| 3-D | three-dimensional |
| AM | additive manufacturing |
| ARL | Army Research Laboratory |
| DEVCOM | US Army Combat Capabilities Development Command |
| EBAM | electron beam AM |
| GVSC | Ground Vehicle Systems Center |
| NDE | nondestructive evaluation |
| SEMD | Sciences of Extreme Materials Division |
| SNR | signal-to-noise ratio |
| WMRD | Weapons and Materials Research Directorate |
| XCT | X-ray computed tomography |

| | |
|---|---|
| 1 (PDF) | DEFENSE TECHNICAL INFORMATION CTR DTIC OCA |
| 1 (PDF) | DEVCOM ARL FCDD RLD DCI TECH LIB |
| 4 (PDF) | DEVCOM ARL FCDD RLW MB W GREEN T WALTER J SIETINS B LOVE |
| 1 (PDF) | DEVCOM GVSC DETROIT ARSENAL D SCHLEH |